Malaysian Journal of Civil Engineering 21(1) : 1- 16 (2009)

GEOSTATIONARY METEOROLOGICAL SATELLITE-BASED QUANTITATIVE RAINFALL ESTIMATION (GMS-RAIN) FOR FLOOD FORECASTING

Wardah Tahir [1], Zaidah Ibrahim [2] and Suzana Ramli [1]

[1] Faculty of Civil Engineering, Universiti Teknologi MARA
[2] Faculty of Computer Science and Mathematics, Universiti Teknologi MARA

Corresponding Author : warda053@salam.uitm.edu.my

Abstract

The consequences of global warming include changes in rainfall patterns and increase in flood risks or droughts. The frequent unexpected climate change phenomena, especially the severe flood occurrences, necessitate improvements in the related weather monitoring instruments and techniques. The rain measuring system, whether the conventional rain gauges or the more advanced Remote Sensing and Transmission Unit (RSTU) panel, can only be sparsely installed at suitable location, hence they are considered as point rain measurement. The paper introduces an innovation to point rain estimation, named GMS-Rain, which estimates convective rainfall using information from the Geostationary Meteorological Satellite-5 (GMS-5) infrared (IR) images and numerical weather prediction (NWP) products in an Artificial Neural Network model. Although the estimates are indirect, meteorological satellites with fine temporal and spatial resolution cover broader areas that may be inaccessible or that may cause difficulties with the traditional rainfall measurement such as the deep forests, large water bodies or rigid mountains, therefore should be taken as complementary to rain gauge or radar measurements. In addition, the rain estimation from the observation of cloud development would enable earlier forecast of critical storm events. The GMS-Rain model is also a potential input to a hydro-meteorological flood forecasting system with an improved lead time of warning. Rainfall estimates from the GMS-Rain are validated against previously recorded hourly and total accumulated Thiessen areal-averaged gauged rainfall values with coefficient correlation values of 0.63 for 0.91 respectively, while an extra lead time of around 2 hours is gained when the model is coupled with a rainfall-runoff model to forecast a flood event in the upper Klang River Basin.

Keywords: *geostationary meteorological satellite; numerical weather prediction; quantitative precipitation forecast; hydro-meteorological; flood forecasting*

1.0 Introduction

Rainfall is one of the most difficult meteorological variables to forecast, due to its large variability both in space and in time. Habets *et al.* (2004) discuss that the potential of numerical weather prediction (NWP) rainfall forecast to be used by hydrological models for flood prediction is constrainted by the three following types of error: (i) localization of the events, since an error of a few kilometers can lead the rainfall in the wrong watershed; (ii) timing of the events, since the response of the basin depends on previous events and on the timing of the present event; and (iii) precipitation intensity. For these reasons, NWP rainfall forecasts are rarely directly used to forecast river-flows. Nakakita (2002;2005) suggests how the quality of rainfall forecasts can be improved spatially or within a smaller grid scale but within a shorter lead time by techniques using satellite and radar data. Figure 1 shows the quality of rainfall forecasts as a function of lead time for several different forecasting methods. NWP would allow greater lead time ahead but in a very coarse scale. Mesoscale numerical and conceptual rainfall models have better spatial resolution but the accuracy may be poorer than the NWP. Extrapolation using satellite and radar observation is capable to produce good prediction within a smaller spatial grid scale but with less lead time.

Numerous studies have been carried out on satellite-based rainfall estimation, among others by Griffith et al. (1978), who have developed the Griffith–Woodley technique.

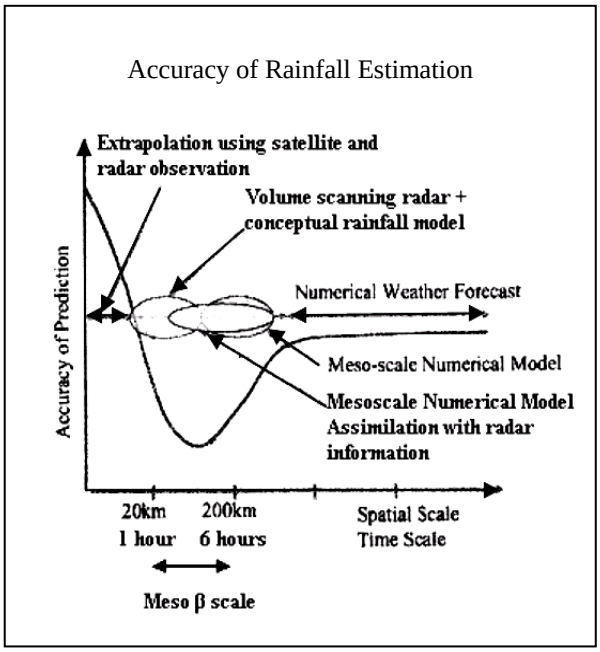

Fig.1: The quality of rainfall prediction as a function of lead time for different forecasting methods (adapted from Nakakita, 2005; 2002)

The technique defines the cloud captured by the satellite image as anything colder than 253 K and estimates the associated radar echo for each cloud. Ba and Nicholson (1998) have used an index of convection based on the METEOSAT IR data and rainfall measurements to analyze the convective activity and its relationship to rainfall. A cloud-indexing algorithms for the polar-orbiting National Oceanic and Atmospheric Administration (NOAA) satellites and for geostationary satellite imagery have been developed by Todd *et al.* (2001). Earlier, Adler and Negri (1988) and Anagnostou *et al.* (1999) have developed a one-dimensional cloud model, which relates the cloud top temperature to the rain rate and rain area; that is called the convective stratiform technique (CST).

Studies on satellite-based rainfall estimation techniques are progressively evolving with the aim of improving accuracy in the rainfall estimates, with a finer spatial and temporal resolution. However, due to the indirect nature of the relationship between the satellite-measured radiance in the infrared regions and the corresponding rainfall, it is observed that the developed techniques are not universally applicable; that is techniques developed for the extratropic regions might not perform well in the tropics. In addition, techniques developed to estimate the monthly rainfall might not be accurate for the hourly rainfall estimation.

2.0 Theoretical background

Convective rain (type of rain which causes flash flood) occurs when heated air is rising and cooled until the condensation occurs and cloud droplets grows then become large enough to fall as rain. The higher the air parcel rise, the colder the cloud temperature. The colder the cloud, the brighter it is on infrared satellite image. Therefore, there is a correlation between cloud top brightness temperatures (Tb) and raining clouds. Thick and tall cumulonimbus clouds which cause flash floods can be identified and detectable in high-resolution infrared images. The cirrus anvils associated with well-developed convection can reach up to 10^5 km^2, and they last long after the actual convection has ceased, whereas the actual deep convection takes place in smaller regions, where the rising air parcels penetrate the entire troposphere in under an hour (van Hees et al., 1999). Griffith et al. (1978) have found that a convective system is more active and produces the greatest rainfall rates when the tops become colder and continue to expand.

In multicell storm as shown in Figure 2, individual thunderstorm cells develop successively at the side of a large storm complex. The systematic development of new cells produces a long-lived storm even though each cell has a limited life cycle (Rogers and Yau, 1996).

At the initial time the storm consists of four cells at different stages of development. The development of the youngest (southernmost) cell at successive times is indicated. The heavy dashed arrow is the trajectory of a parcel in the growing cell.

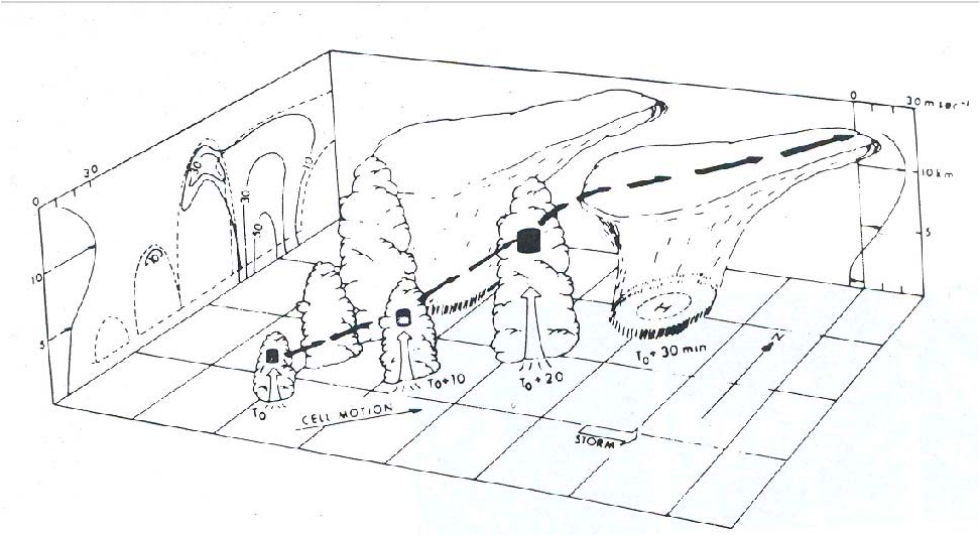

Figure 2 : Schematic view of a multicell storm (Rogers and Yau, 1996)

3.0 Research methodology

The methodology is described briefly in the paper. The detail methodology can be referred from Wardah *et al.* (2008).

3.1 Data collection

The data acquired to be used in the development of the GMS-Rain are as listed below:

i. Hourly infrared GMS-5 and MTSAT images (example image is given in Fig.3) from year 2003 and wet days from 2004-2006 (features of clouds are correlated with the rainfalls)
ii. Weather radar display images and reflectivity (verified with gauged-measured rain)
iii. Numerical weather prediction model products (relative humidity, precipitable water content, vertical wind)
iv. Rainfall and runoff data (include catchment characteristics)

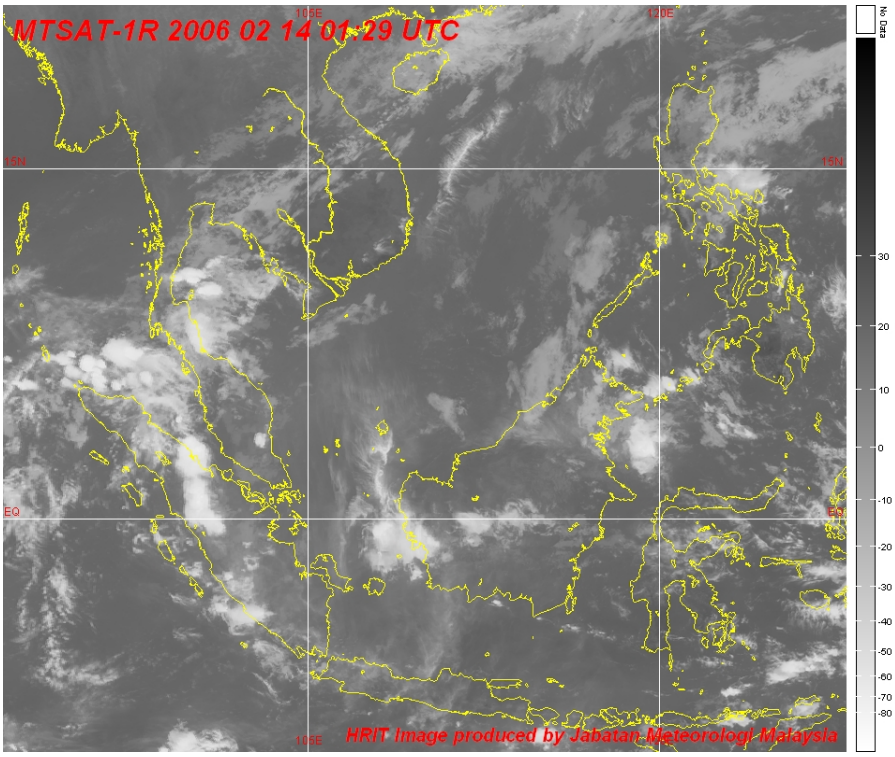

Figure 3 : An example of an infrared MTSAT (Multifunctional Transport Satellite) image (latest generation of GMS-5)

Following Kidder and Vonder Haar (1995), there are two ways of verifying rainfall estimates from satellite image that are (i) comparing with rain gauge values and (ii) comparing with radar rain estimates. Comparison of satellite rain estimates with radar is considered more reasonable since it samples an area comparable with the size of satellite pixels; even though generally radar rain estimation is less accurate than the rain gauge measurement. Comparison of satellite rain estimates with rain gauge would be poor due to the high spatial variability of rain since rain gauge samples area roughly 0.1 m in diameter. Because radar technique is also an indirect estimation of rain rate, a verification procedure of the technique had been performed beforehand by comparing radar rain estimation with point rain gauge measurement.

3.2 GMS-Rain development using the Artificial Neural Network Model.

Eight variables with direct and indirect correlation with the radar rain rate are trained with the radar rain rate in a back-propagation neural network. The eight variables are (i) satellite infrared cloud top brightness temperature (Tb), (ii) standard deviation and (iii) mean Tb of 5x5 pixels, (iv) Tb change (v) sobel operator to indicate gradient, (vi) precipitable water content, (vii) relative humidity and (viii) vertical wind.

The training process requires a set of examples of proper network behaviour – network inputs, and target outputs. During training, the weights and biases of the network are iteratively adjusted to minimize the average squared error between the network outputs and the target outputs. The input variables are trained against the rain-gauged verified radar rain rate. A set of 204 data have been retrieved for convective rain events and are used in the training process. The optimum ANN structure was determined by varying the number of neurons in each layer to determine the structure that gives the best model performance. The final network consists of an input layer with eight input variables, one hidden layer with three neurons, and one output layer as indicated in Figure 4. The output of the model is the rain rate (mm/h) at the collocated time of the satellite images.

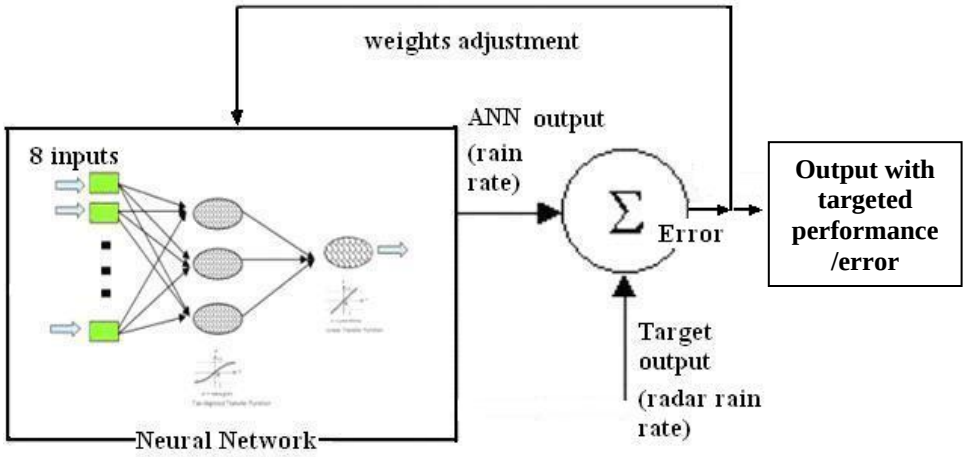

Figure 4: The back-propagation neural network with the inputs and outputs

4.0 Results and discussion

4.1 Model application

The ANN model for satellite rainfall estimation is applied to estimate the areal rainfall in the upper Klang River Basin by repeated runs on every pixel covering the area. An example is shown in Figure 5 for the rainfall estimation during a flash flood event, dated June 10, 2003

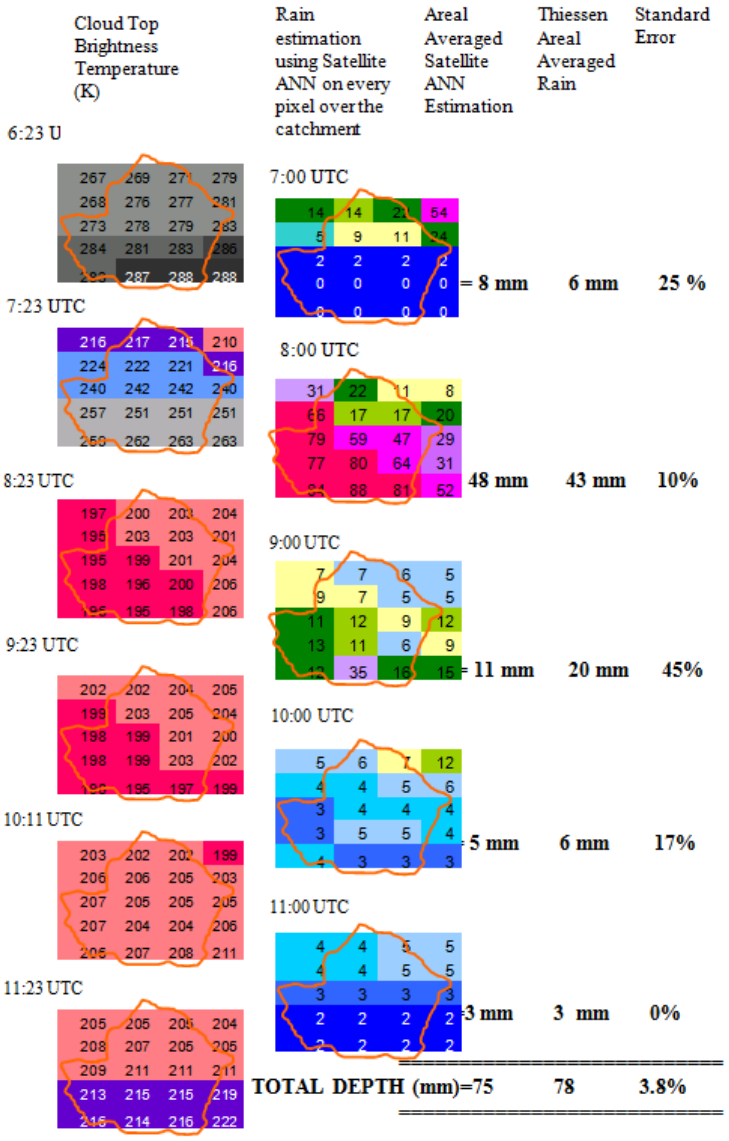

Figure 5 : June 10, 2003 rain estimation using the ANN based technique

The first column consists of pixel representations over the catchment, which have been arranged in time sequence with the cloud-top brightness-temperature assigned using a program developed using MATLAB™ image processing tool. The second column is the estimated rainfall rate for each pixel for the given durations. Note that one of the input variables to the ANN model is the temperature change per hour, thus two images in time

sequence are required to calculate the variable. Since the output from the model is the rain rate for each pixel in mm/h, the areal-averaged rain depth for the corresponding hour can then be estimated by arithmetic average of all the pixels involved. Apparently, the technique has performed well in estimating the flash-flood event on June 10, 2003 with a total standard error of 3.8% .

4.2 Model validation

This study regards the use of gauged rainfall measurements as the 'truth'; hence, it uses them for validation purposes. Hourly rainfall data have been collected from the DID of Malaysia for ten stations in the upper Klang River Basin, as shown in Figure 6.

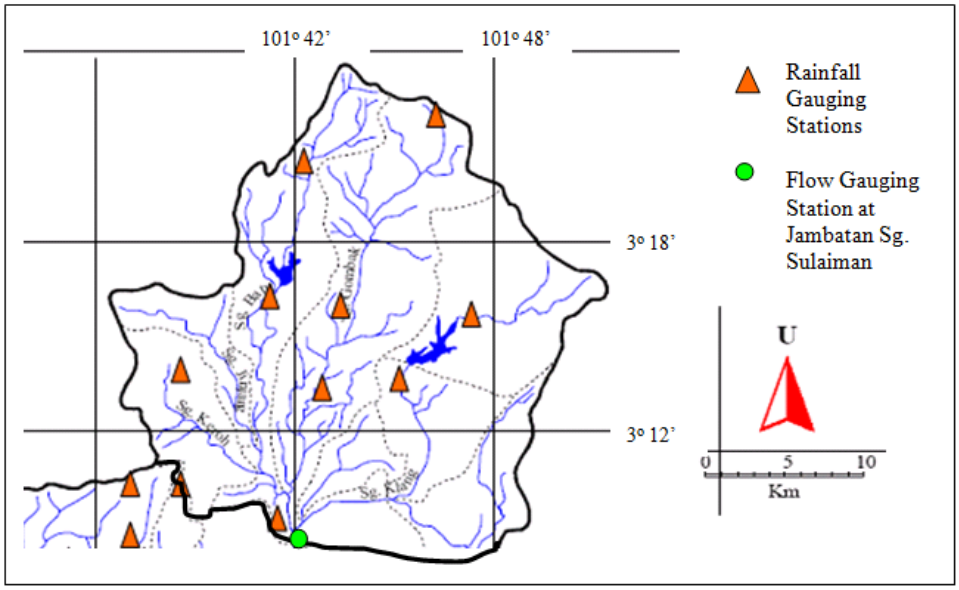

Figure 6: The upper Klang river basin

Convective rainfall events of the heavy category (>30mm/h) for at least one station are selected from the year 2006 and from the wet months of 2005 for validation purposes. A total of 107 hourly rainfall data sets from 33 storm events have been selected. To measure the validity of the satellite rainfall estimation values obtained by the ANN model to the gauged rainfall values, the correlation coefficient, *r*, has been determined. An *r* value of 0.63 is obtained, which indicates that there is relatively weak correlation between the hourly areal-averaged rain estimation using the ANN model versus the gauge-measured Thiessen areal-averaged rain. The results improved encouragingly for the total areal averaged rain depth estimation with *r* value of 0.91 as indicated in Figure 7. The storm events included here are 2-h, 3-h, and 4-h rainfall.

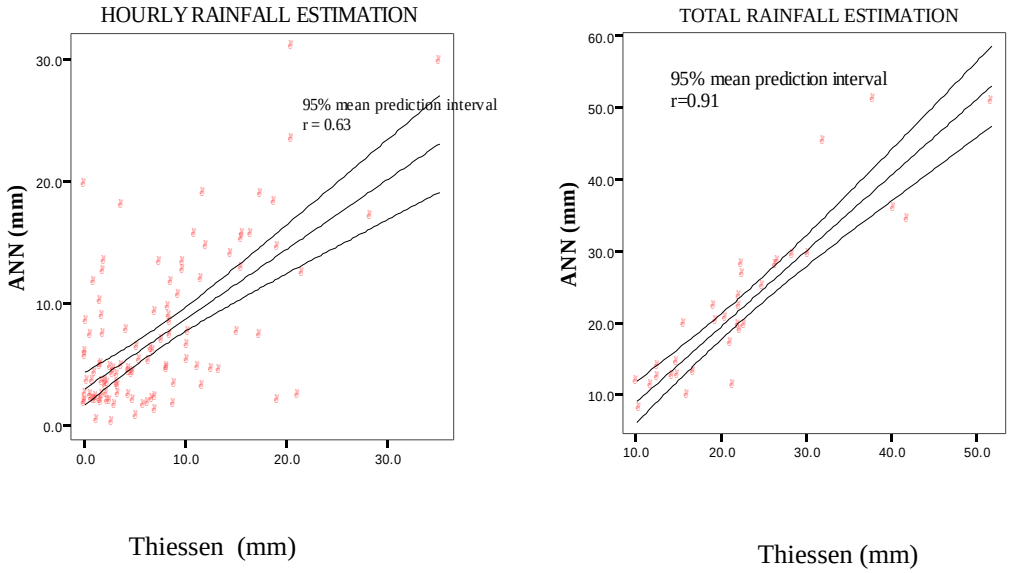

Figure 7: Validation of areal-averaged rainfall estimation by the GMS-Rain against gauge-measured Thiessen areal-averaged rain

Other accuracy measures carried out in the study are the determination of mean absolute error (MAE) and root mean squared error (RMSE). The values of MAE and RMSE for the hourly estimation using the ANN model are 3.8 and 5.6, respectively, whereas the same values for the total rainfall estimation are 3.3 and 4.7, respectively. The values are considered satisfactory within a corollary that better estimation is expected for longer time duration

4.3 Quantitative Precipitation Forecast (QPF)

In addition to being a significant complementary tool to rain-gauge measurement and radar estimation, satellite-based rainfall estimation can be enhanced as a quantitative precipitation forecast (QPF).

The rainfall estimation can become a rainfall forecast only when the future movement of rain can be predicted. The QPF can then be considered as an input to a flood forecasting system so as to gain an improved lead time.

In this study, a cross-correlation *(r_{xy})* technique is applied to track the cloud cell movement to develop a QPF as suggested by Kidder and Vonder Haar (1995). The method allows for calculation of the average motion of an area of clouds in which two time sequence images are needed. A target array which contains the convective cloud cell is selected for the first image.

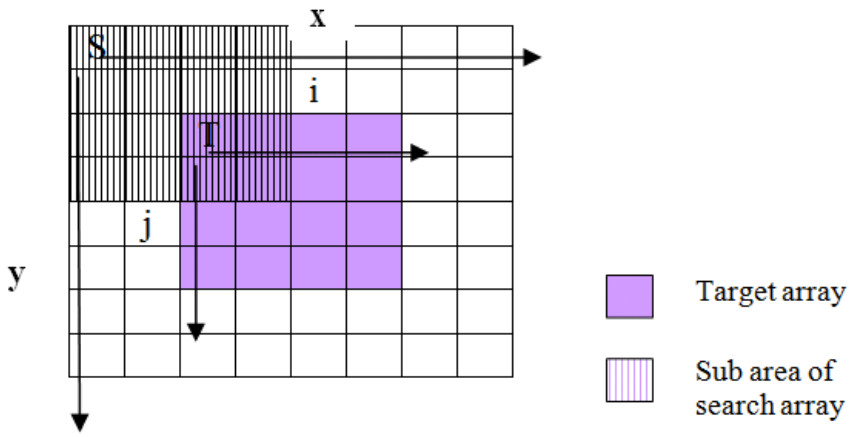

Figure 8: Illustration of the cross-correlation technique

$$r_{x,y} = \frac{\sum_{i=1}^{4}\sum_{j=1}^{4}[S_{i+x+2,j+y+2} - \bar{S}(x,y)][T_{i,j} - \bar{T}]}{\left\{\sum_{i=1}^{4}\sum_{j=1}^{4}[S_{i+x+2,j+y+2} - \bar{S}(x,y)]^2 \sum_{i=1}^{4}\sum_{j=1}^{4}(T_{i,j} - \bar{T})^2\right\}^{1/2}} \qquad \text{Eq. 1}$$

Then, assuming that the clouds have moved, but changed little, during the time interval between the time sequence images, the cross-correlation technique is applied to locate this area in the second image as shown in Fig.8 and calculation of r_{xy} is given by Eq.1. The direction of the cloud cell movement will be indicated by the largest r value.

4.4 Application of the model for flood forecasting

The cloud cells are tracked during their movement using a cross-correlation technique, and rain can be forecasted about 2 h earlier, as described in a case study of the June 10, 2003 flash-flood event. The QPF has been coupled with the catchment average unit hydrograph (UH). Figure 9 shows the hydrographs of the forecasted flow versus the actual observed flow. At time 16:00 h, it can be forecasted that a peak flow of around 500 m^3/s is about to occur at the flow-gauging station 2 h later (around 18:00 h). The observed flow record shows that an actual peak flow of around 556 m^3/s had actually occurred at about 18:00 h; therefore, an extra lead time of 2 h has been gained using the satellite-based rainfall forecast. Consequently, a total of approximately four hours of lead time (from the time of rain centroid) has been attained by coupling the satellite-based rainfall forecast and the UH technique.

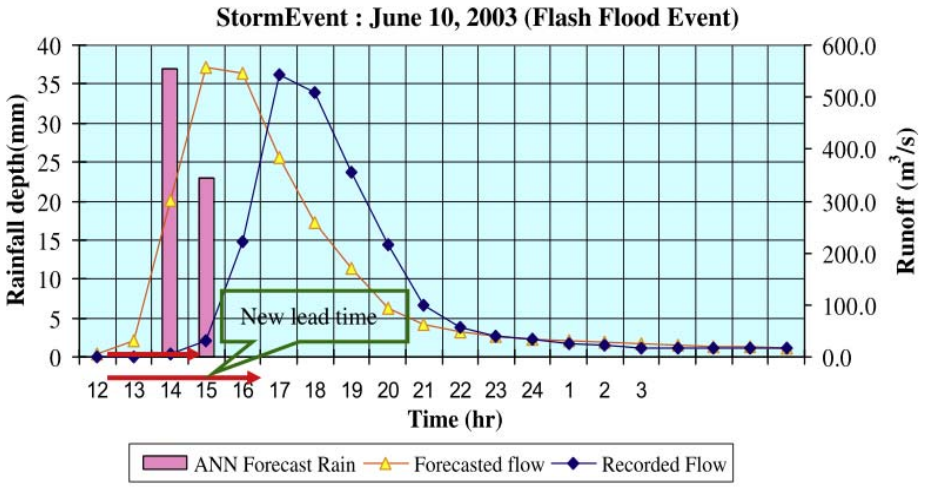

Figure 9: Forecasted flow plotted against the observed flow with the new lead time

Figure 10 shows a flowchart illustrating the whole process of rainfall forecasting using the satellite-based rainfall estimation and coupling the QPF with a rainfall-runoff model; an example of a rainfall-runoff model used in the study is the unit hydrograph method.

5.0 GMS-Rain Interface

Using MATLAB™, a Graphical User Interface (GUI) setup has been developed for the satellite based rainfall estimation using the ANN technique. The application package is then named the GMS-Rain. Figure 11 shows the main application page of the GMS-Rain. The interface first requests the user to enter the satellite image. The user would then have to select the area of interest for rainfall estimation. Once the area has been selected, it will zoom for better view of the pixels. At this stage, the background map for river basins in Peninsular Malaysia will appear for convenient comparison with the satellite image and location search. Next the user will have to input the three numerical weather prediction forecast values namely the precipitable water content (PW), relative humidity (RH) and vertical wind (VW) as indicated by Figure 12. Pressing the neural network button will perform the rainfall estimation by the ANN model. The results will be indicated by certain colors for certain range of rainfall intensity on the pixels of the interest area on the satellite image as shown in Figure 13. The average rain depth over the pixels of the interest area will be displayed under the result image.

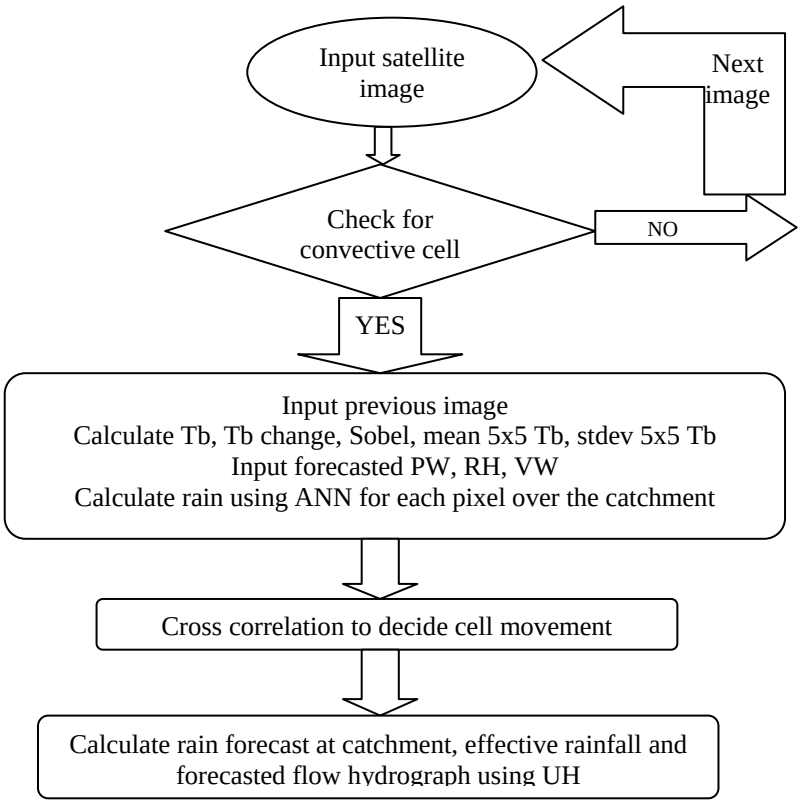

Figure 10: The flowchart on coupling the satellite-based rainfall estimation model with rainfall-runoff model (UH).

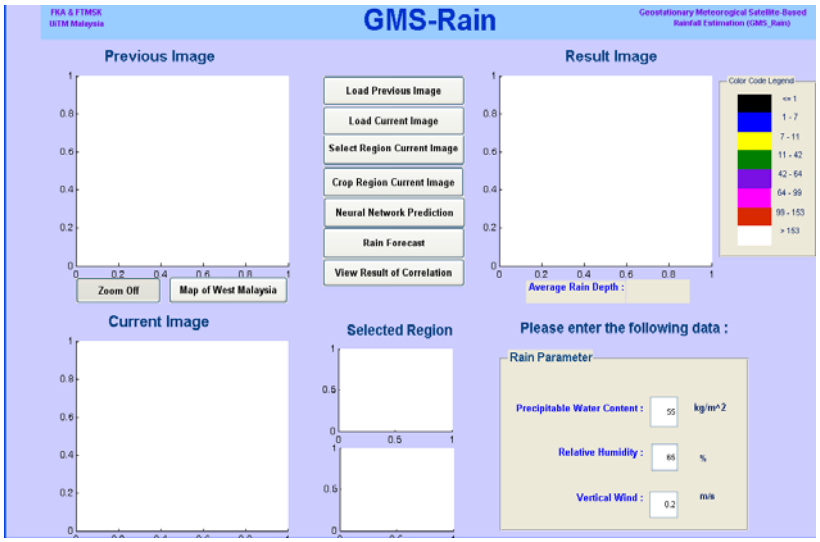

Figure 11 : Main interface of GMS-Rain

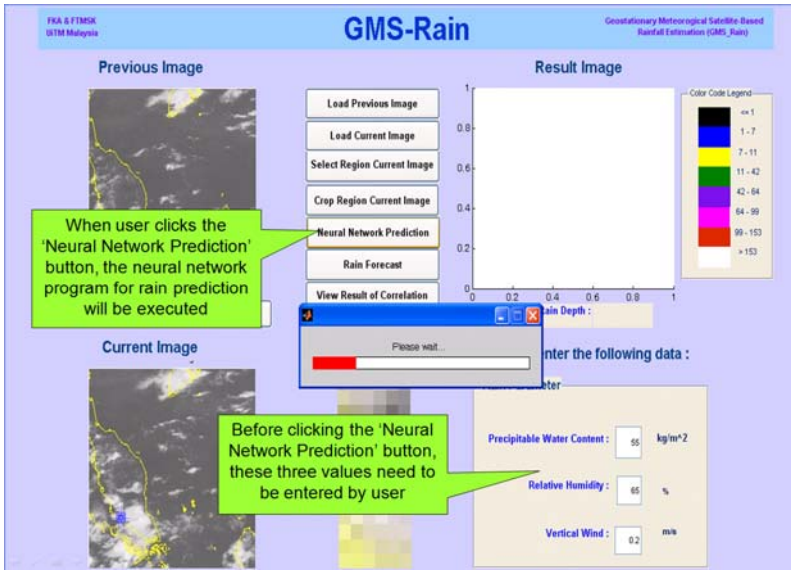

Figure 12 : Rainfall estimation steps using the GMS-Rain

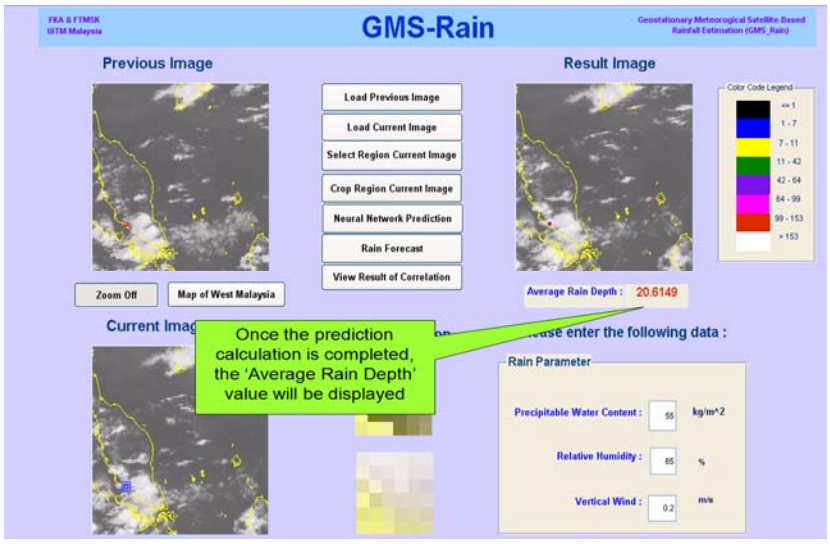

Figure 13 : Display of results in color range rainfall intensity of the pixels over the selected area and average rain depth value.

The rainfall forecast algorithm by the cross correlation technique can also be executed by choosing the *Rainfall Forecast* button. This algorithm will result in the direction of the cloud cell movement as shown in Figure 14.

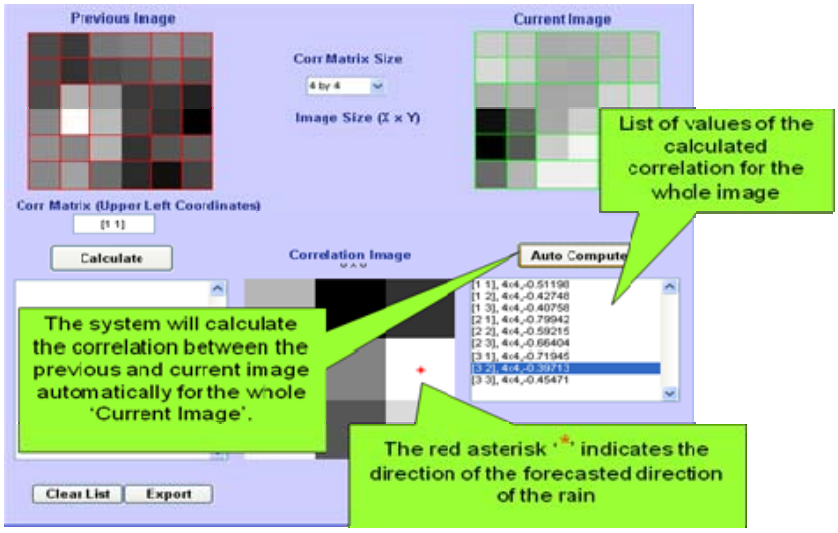

Figure 14: Rainfall forecast using the cross-correlation technique in GMS-Rain

4.0 GMS-Rain Real-Time Application

GMS-Rain can be potentially applied in a coupled hydro-meteorological flood forecasting system which operates in real-time basis to forecast and provide an early warning to citizen living in the flood-prone areas. To work the model in real-time, it has to be run at the location where the IR images are received, such as at the Malaysian Meteorological Department (MMD) Headquarters. Immediately after the IR image for the hour is received, it will be fed into the GMS-Rain for areal-averaged rainfall estimation, focusing on the catchment area of interest. The cross-correlation technique will be applied to track the cloud cell movement. If the movement is proceeding in the direction towards the monitored catchment, as can be determined from the image in time sequence, the rain estimation can then be coupled with the available rainfall-runoff model of the catchment, for flood forecasting.

The MMD received more than one type of image (e.g.: MTSAT from Japan and FY-2C from China) within half an hour interval, therefore the use of several type of images may produce a more convincing rainfall estimation. In addition, forecast values of the PW, RH and VW need to be acquired on time, thus NWP products applied by the MMD have to be used. If the satellite images and the NWP products are received real-time, it is possible to achieve real-time rainfall and flood forecasting.

5.0 Conclusion

The main contribution of this work is the development of the geostationary meteorological satellite-based convective rainfall estimation model for an equatorial country such as Malaysia. The model has been developed by incorporating the knowledge from actual observations after thorough exploratory and correlation analysis between the geostationary meteorological satellite IR images and intense convective rain. The model performed satisfactorily in estimating the areal-averaged rainfall depth for convective rain events in a given duration, and the results output have been validated against the gauged rainfall. A value of 4.7 for the RMSE can be considered as a typical magnitude for an error in estimation (Wilks, 1995). Hence, if the rain estimation is 30 mm, and error of 16% is expected in the estimation. Further comprehensive work is required for the establishment of this rainfall-estimation model as a reliable quantitative rainfall forecast that can be used as input to a flood forecasting-and-warning system with a better lead time.

Acknowledgements

The author would like to thank the Research Management Institute of Universiti Teknologi MARA for funding the project, the Head of Satellite Divison from the Malaysian Meteorological Department and many helpful individuals from the Drainage and Irrigation Department. We are grateful to an anonymous reviewer for providing comments that considerably improve the manuscript.

References

Adler, R. F., and Negri, A.J. (1988). A satellite infrared technique to estimate tropical convective and stratiform rainfall. *Journal of Applied Meteorology*, 27, pp. 30-51.

Anagnostou, E. N., Negri, A.J., and Adler, R.F. (1999). A satellite infrared technique for diurnal rainfall variability studies. *Journal of Geophysical Research*, 104, pp. 31477–31488.

Ba, M. B., and Nicholson, S. E. (1998). Analysis of convective activity and its relationship to the rainfall over the Rift Valley lakes of East Africa during 1983-90 using the Meteosat infrared channel. *Journal of Applied Meteorology*, 37, pp. 1250-1264.

Griffith, C. G., Woodley, W. L., Grube, P. G., Martin, D.W., Stout, J., and Sikdar, D.N. (1978). Rain estimation from geo synchronous satellite imagery - Visible and infrared studies. *Monthly Weather Review*, 106, pp. 1153-1171.

Habets, F., LeMoigne, P., and Noilhan, J. (2004) On the utility of operational precipitation forecasts to served as input for streamflow forecasting, *Journal of Hydrology* , 293 , pp. 270–288.

Kidder, S.Q and Vonder Haar, T.H (1995) Satellite Meteorology, An Introduction, Academic Press.

Nakakita, E. (2005). Personal Communication, Professor of Hydro-meteorology, Disaster Prevention Research Institute (DPRI), Kyoto University, Japan.

Nakakita , E. (2002). Radar Hydrology Precipitation and Water Resources. *Textbook for 12th IHP Training Course*, HyARC Nagoya University and UNESCO pp. 111-129.

Rogers, R.R., Yau, M.K., 1988. A Short Course in Cloud Physics.Butterworth-Heinemann, p. 290.

Todd, M. C., Kidd, C., Kniveton, D., and Bellerby, T.J.(2001). A combined satellite infrared and passive microwave technique for estimation of small-scale rainfall. *Journal of Atmospheric and Oceanic Technology*, 18, pp. 742-755.

van Hees, R.M., Lelieveld, J., Collins, W.D., (1999). Detecting tropical convection using AVHRR satellite data. *Journal of Geophysical Research*, 9213–9228.

Wardah, T., Abu Bakar S. H., Bardossy, A. , and Maznorizan M. (2008). Use of Geostationary Meteorological Satellite Images in Convective Rain Estimation for Flash-Flood Forecasting. *Journal of Hydrology*, 356, pp. 283– 298.

Wilks, D.S., (1995). Statistical Methods in the Atmospheric Science. Academic Press, pp. 233–281.